

## CHAPTER 3

### RESULTS AND DISCUSSION

As stated earlier that the purpose of this research would concentrate on the characterization of the prepared hydrogels, so after the SF films and SF hydrogel films were prepared, the results on their properties that were characterized using various techniques are as follows:

#### 3.1 Preparation of the SF Films

The preparation of SF films was done step by step. Firstly, the silk powder was prepared by degumming the silk waste obtained from silk reeling process to remove a sericin coated on the silk fiber and some contaminated substances. Next, the degummed silk fiber was dissolved in a mixed solution of  $\text{CaCl}_2$ , ethanol and water, then purified by dialysis for 3 days. After that the SF solution was freeze-dried to obtain SF powder. Finally the SF powder was dissolved in deionized-reversed osmosis (DI-RO) water then poured the SF solution into a PE plate and dried in oven at 60 °C for 12 hrs to obtain SF films. The preparation processes are depicted as shown in **Fig. 3.1** and **Fig. 3.2**.

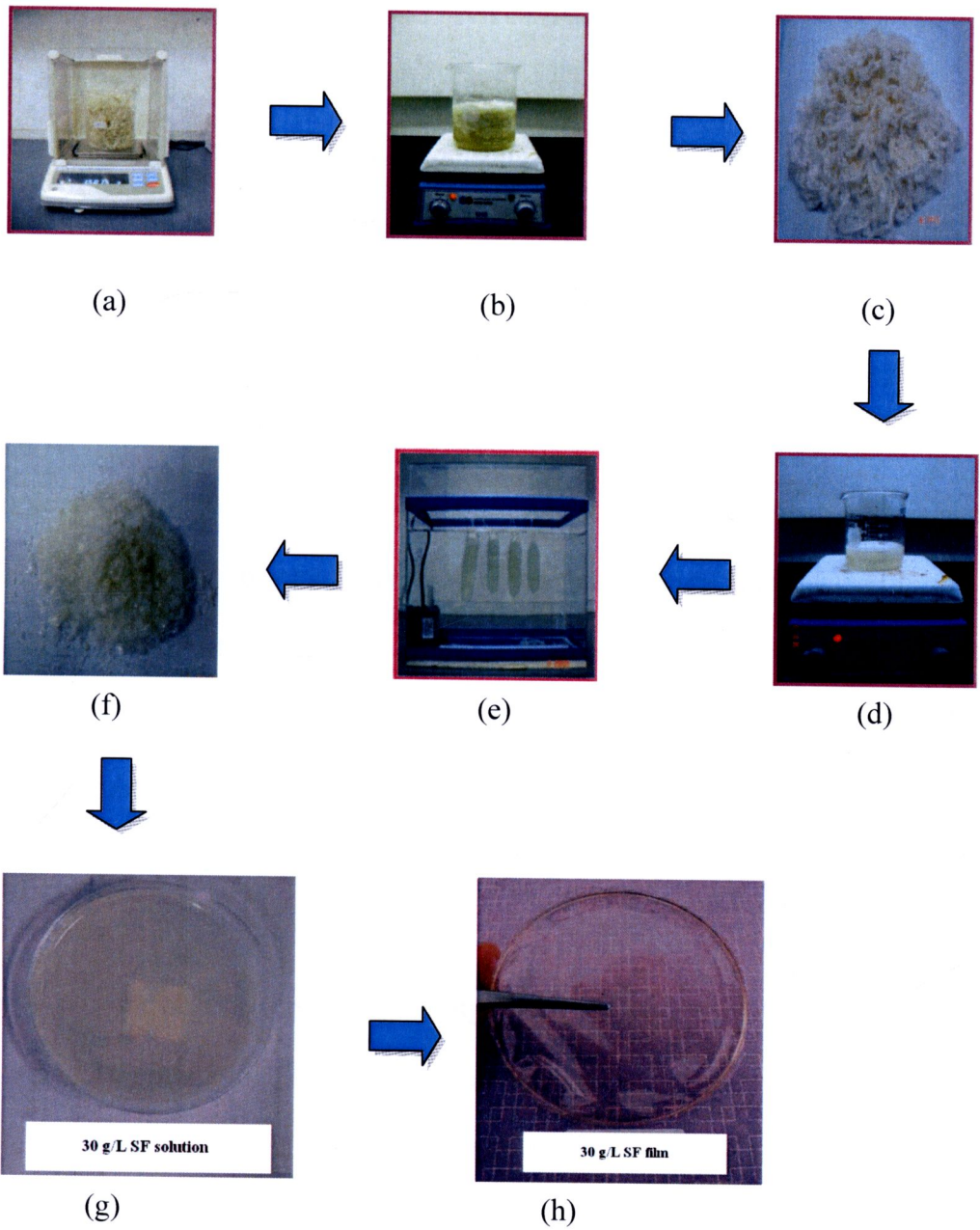


**Fig. 3.1** Preparation of SF film: (a) silk waste, (b) degumming, (c) degummed silk, (d) dissolution, (e) dialysis, (f) SF powder, (g) 30 g/L SF solution and (h) 30 g/L SF film

Generally, the degumming of silk has been carried out for many years in alkaline solution. Sericin is a water soluble protein and can be degraded through hydrolysis when sericin is dissolved in acid or alkaline solutions. On the other hand, fibroin is insoluble in alkaline while sericin is soluble. A weight loss of sericin, about 22-25%, occurs during the degumming process [44]. The insoluble silk was removed from boiling alkaline solution, wrung out and rinsed thoroughly in DI-RO water facilitated the removal of more water-soluble sericin fraction. In this study,  $\text{Na}_2\text{CO}_3$  solution was used as an alkaline solution to remove glue-like sericin and solubilize in solution and followed by dialysis to remove salt. A higher temperature was selected in the range of 110-115°C. At the heating temperature which is lower than 110 °C, the degummed SF fiber was hardly dissolved. This is because, the larger of sericin peptides are soluble in hot water and the bubbles occurred in the solution with high evaporation rate of solvent at the lower heating temperature higher than 115 °C could also be observed.

The SF powder obtained by freeze-drying appears to be pale yellow and slightly flaky in **Fig. 3.1(f)** while the SF solution was yellowish and slightly turbid. A dried SF film is transparent, rigid and brittle as illustrated in **Fig. 3.1(g-h)**.

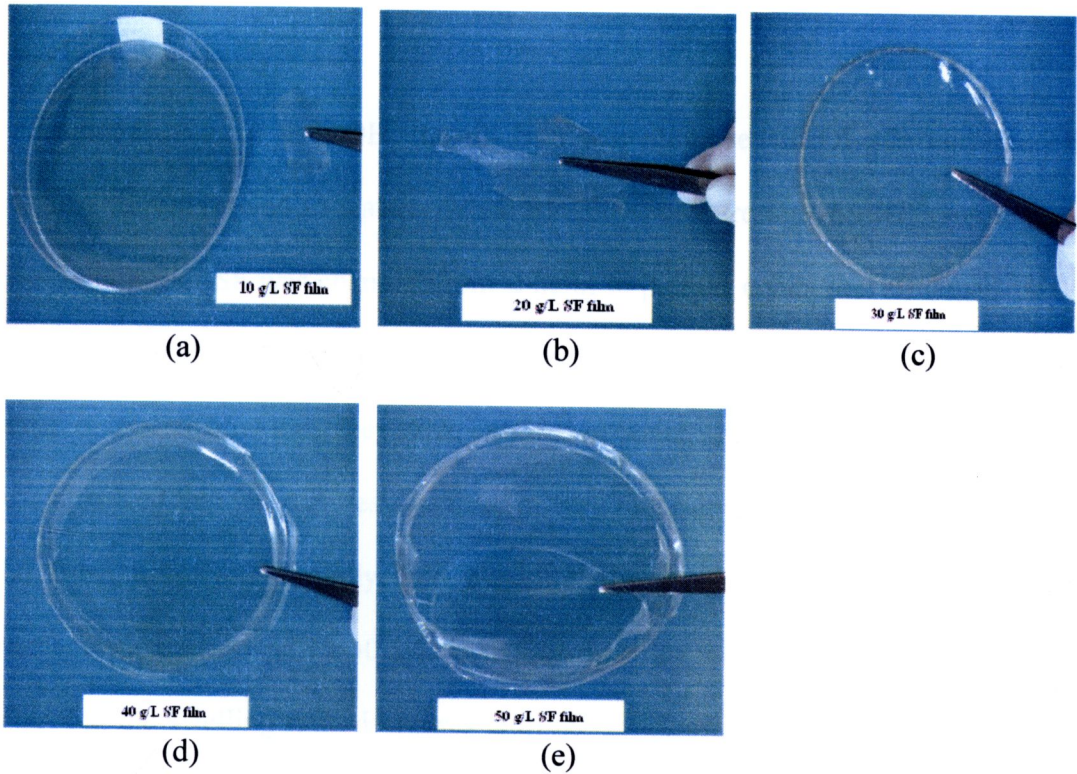


**Fig. 3.2** Photographs of SF films prepared from SF solutions at various concentrations: (a) 10 g/L, (b) 20 g/L, (c) 30 g/L, (d) 40 g/L and (e) 50 g/L of SF films

**Fig. 3.2**, shows the appearance of the SF film that were prepared at various concentrations ranging from 10-50 g/L. The SF films exhibit their transparency, it can be observed that the color of the films becomes more yellowish and opaque as the concentrations of fibroin increase. During the film forming process, the films were casted restrictly only in PE plate with 9 cm internal diameter to accommodate 30 mL volume of the mixtures. It was observed that the films formed from the mixtures with concentrations of 10 and 20 g/L were not in good film shapes; too thin and torn. Whereas the films prepared from 40-50 g/L mixtures were too hard and brittle.

Therefore, the SF film of 30 g/L mixture was the best physical condition that can be used for further study.

After treating with EtOH, the SF film was immersed in DI-RO water and the swollen film dissolved in water. When SF films were treated in EtOH solution, the conformation of SF was changed from  $\alpha$ -helix to  $\beta$ -sheet crystalline structure. It was observed that if the films were insoluble in water then they would not interact with water no matter how long they were exposed in water. In the case of soluble films, it was observed that the samples dissolved at very first minutes of immersion or some of the films dissolved partially. In **Fig. 3.3**, the swelling ratio of SF films with concentration range of 10-30 g/L increases with an increase of SF concentrations, after that the swelling ratio decreases until the concentrations are up to 50 g/L of SF. This happening is because at high concentration of SF, it forms a dense outer layer and decreases pore size, thus restricting the access of water molecules through the SF films. Therefore the relationship among the drying films, swelling ratio and physical properties of SF film can be combined for considering on selecting 30 g/L to be optimum concentration for film production.

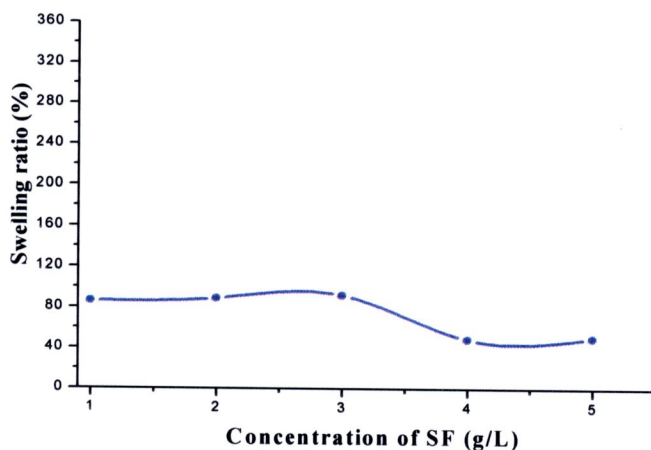


**Fig. 3.3** The swelling ratio of SF films at various concentrations of SF solutions

### 3.2 Preparation of the SF Based Hydrogel

Improvement of mechanical properties of the SF film was carried out by blending SF with gel formers. The obtained hydrogel films exhibit their transparent characters as shown in **Fig. 3.4**.

In **Fig. 3.4(a)**, the effect of EtOH treatment on the SF hydrogels reveals that the film becomes more rigid and brittle. Aqueous EtOH treatment has been found to cause  $\beta$ -sheet formation in this material. Such transformation is known to be effective in improving the physical strength and water resistance of SF-based biomaterials [45].

Upon adding Carbopol (CP) as a gel former (**Fig. 3.4(b)**), the mixtures were allowed to settle to let the air bubble escape for 1 hr and then neutralized with 1 mL triethanolamine (TEA) to thicken the gels. The TEA solution is not used to thicken the gel of Poloxamer and HPMC. The reason that TEA is only used in helping CP to dissolve because TEA will act as a neutralizing agent, so TEA was added until a required pH of solution (pH 6-7) is achieved. Due to the CP, as supplied, are dry and tightly coiled acidic molecules, when it is dispersed in water, the molecules begin to be hydrated and partially uncoiled. The most common way to achieve maximum thickening form of CP is by converting the acidic CP to salt. Neutralization is necessary to fully open the polymer to achieve maximum thickening, suspending and possible emulsion stabilization properties [46]. All obtained gels were visually observed for their physical appearances, i.e., clearness, color and homogeneity.

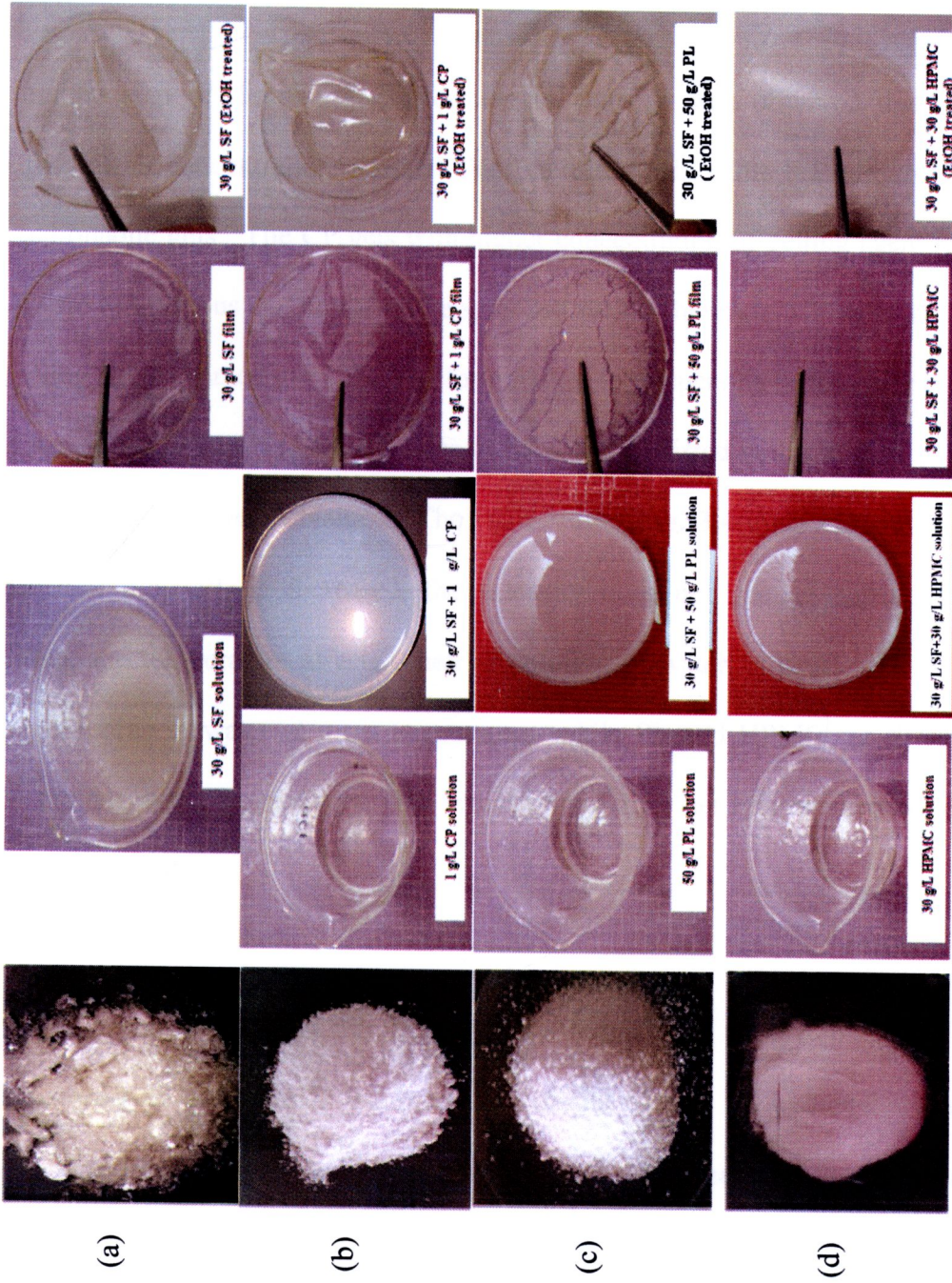


**Fig. 3.4** Appearance illustrating of the SF films and SF hydrogel films; (a) SF, (b) SF/CP, (c) SF/PL and (d) SF/HPAIC

By comparing the physical appearances of the prepared SF-gel former hydrogels, the SF/CP hydrogel (**Fig. 3.4(b)**) was transparent whereas the SF/HPMC hydrogels formed turbid film and the SF/PL film was turbid white. However, when the SF “only” hydrogels were treated with EtOH, the films were deformed and cracked in dry state.

In the step of dissolving gel formers in water it was observed that HPMC mixtures at all concentrations formed clear colorless gels while the mixtures of CP formed opaque gels. The CP gels with higher concentration of gelling agent (50- 60 g/L) were too viscous and could not be spreaded well. Therefore, CP gel with 10 g/L of gelling agent seemed to be the best formulation for dispersing in the solvent. TEA was subsequently added to the mixtures of SF and CP, stirred with a stirring rod until homogeneous gels were obtained. The PL mixture (**Fig. 3.4(c)**) is clear even when concentration of PL is increased, the viscosity does not change apparently. In addition, the temperature affected their dissolution in water as usual. The CP can easily dissolve in water at room temperature, while PL and HPMC can dissolve in cold and hot water, respectively. The viscosity of gel former mixtures are as follows: CP > HPMC > PL.

### 3.3 Characterization of SF Films and SF Hydrogels

In order to characterize the properties of the treated SF hydrogel films with various gel formers, FTIR and DSC analyses were performed and the results are as follows:

### 3.3.1 Cross-linking investigation

FT-IR spectrometry was used to characterize the secondary structure of the SF hydrogels with gel formers and the powder of the samples. The operation was carried out at room temperature using the KBr disk method after the sample had been prepared. The FTIR spectrum of each sample was obtained in the region of 4000-400  $\text{cm}^{-1}$ . The SF hydrogel structures were investigated in terms of amide peaks present in the IR spectra. FTIR spectra of pure components and different compositions of SF and gel formers blend are shown in **Figs. 3.5, 3.7, 3.9** and absorption frequencies of the characteristic bands of SF and gel formers are summarized in **Tables 3.1-3.3**.

#### 1) SF/CP hydrogel

**Fig. 3.5(a)** shows the absorption bands of the SF powder of which the absorptions at 1687, 1526 and 1239  $\text{cm}^{-1}$  are assigned to amide I, amide II and amide III respectively. These bands reflect the existence of random coil structure. The absorption bands of EtOH-treated SF films have frequencies at 1663  $\text{cm}^{-1}$  (amide I), 1553  $\text{cm}^{-1}$  (amide II) and 1232  $\text{cm}^{-1}$  (amide III) which are the characteristics of  $\beta$ -sheet conformation, as shown in **Fig. 3.5(b)**.

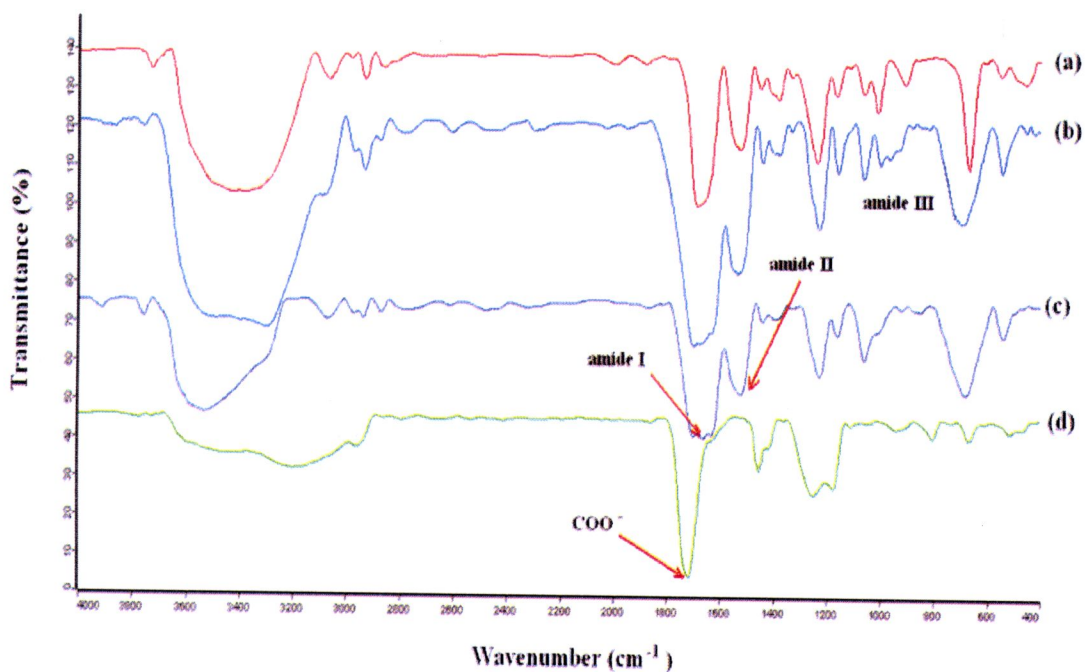


**Fig. 3.5** FTIR spectra of (a) SF powder, (b) SF hydrogel, (c) SF/CP hydrogel and (d) CP powder

In addition, the SF/CP blend also exhibits absorption bands (**Fig. 3.5(c)**) at  $1662\text{ cm}^{-1}$  (amide I),  $1525\text{ cm}^{-1}$  (amide II) and  $1228\text{ cm}^{-1}$  (amide III), which are the characteristic absorption of  $\beta$ -sheet structure of SF, and the corresponding band intensities increase with the increase of interaction between SF and CP. This band tends to move to a higher vibrational frequency with the presence of CP composition, which indicates the change of acid-acid intramolecular hydrogen bonding of CP by the acid-amine bonding of SF/CP blend (**Fig. 3.6**) [35].

In the CP spectrum (**Fig. 3.5(d)**), a broad and intense band of pure CP was observed. This band corresponds to the overlap of two bands at  $3599\text{ cm}^{-1}$  and  $3195\text{ cm}^{-1}$  which is related to the free hydroxyl group and the hydroxyl-forming intermolecular hydrogen bonding, respectively. The strong band at  $1715\text{ cm}^{-1}$  is due

to the carbonyl stretching of the carboxylic group of the CP polymer (**Fig. 3.5**). The resulting observation might be interpreted as the interaction between SF and CP could be between the hydroxyls of amino acids of SF and the  $\text{COO}^-$  group of CP when pH of the solution is between 6-7.

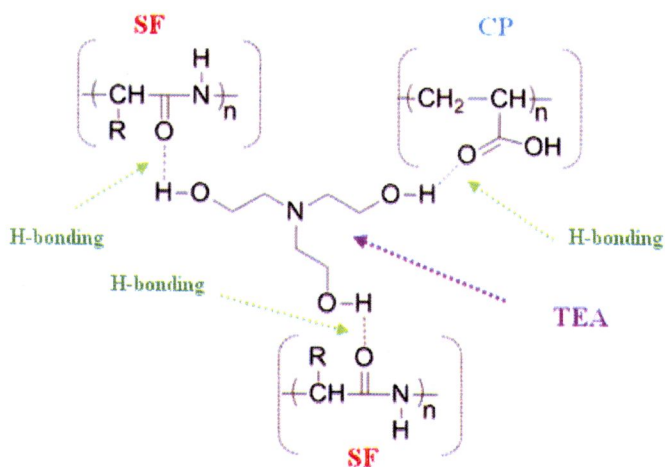


**Fig. 3.6** Intermolecular interaction between SF, Carbopol and triethanolamine

The absorption frequencies of the characteristic bands of SF powder, Carbopol powder, SF hydrogel and SF/CP hydrogel are summarized in **Tables 3.1**.

**Table 3.1** Characteristic IR bands of SF powder, SF hydrogel, SF/ CP hydrogel and CP powder

| <b>Sample</b>  | <b>Observed frequency<br/>(<math>\text{cm}^{-1}</math>)</b> | <b>Assigned absorption<br/>bands</b> |
|----------------|---|--------------------------------------|
| SF powder      | 1687  | C=O stretching                       |
|                | 1526  | N-H bending                          |
|                | 1239  | C-N stretching                       |
| SF hydrogel    | 1663  | C=O stretching                       |
|                | 1533  | N-H bending                          |
|                | 1239  | C-N stretching                       |
| SF/CP hydrogel | 1663  | C=O stretching                       |
|                | 1523  | N-H bending                          |
|                | 1228  | C-N stretching                       |
| CP powder      | 1715  | C=O stretching                       |
|                | 3599  | O-H stretching                       |
|                | 3195  | O-H stretching                       |

## 2) SF/PL hydrogel

Once the FTIR of SF/PL hydrogel was recorded in order to investigate its structures using the knowledge of vibration origin of amide bond and others to study the molecular conformation as shown in **Fig. 3.7**.

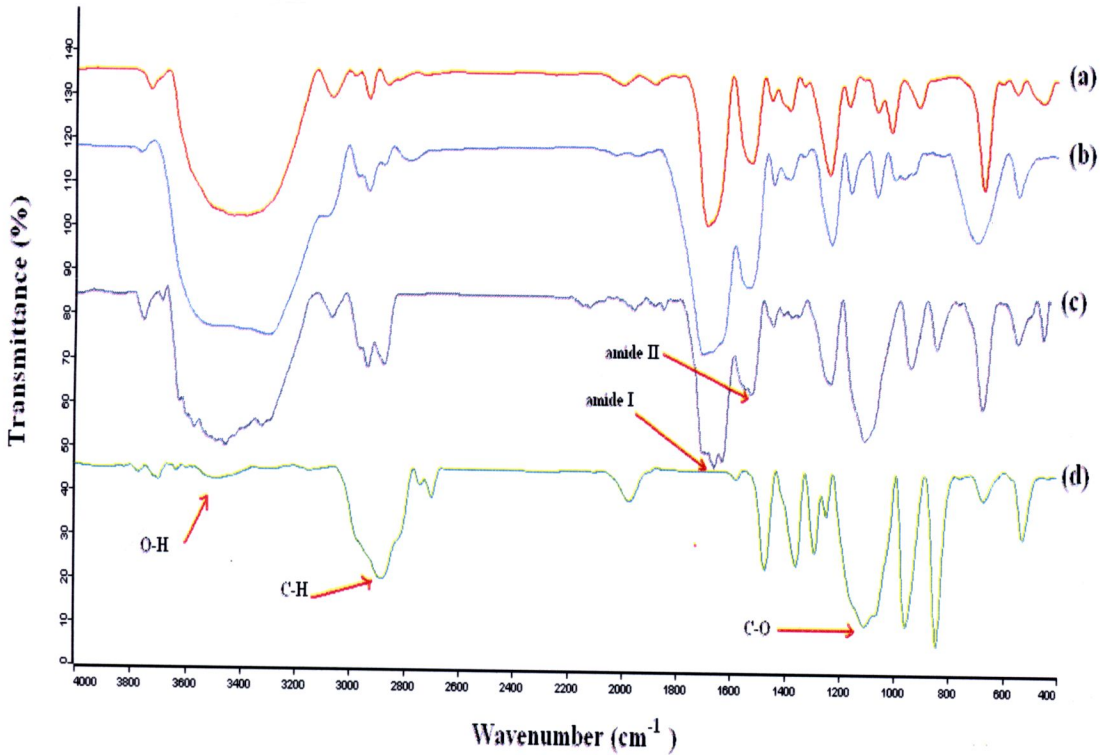


**Fig. 3.7** FTIR spectra of (a) SF powder, (b) SF hydrogel, (c) SF/PL hydrogel and (d) PL powder

FTIR spectrum of PL 188 (**Fig. 3.7(d)**) exhibits characteristic IR bands at  $3495\text{ cm}^{-1}$  (broad),  $2885\text{ cm}^{-1}$  (intense) and  $1106\text{ cm}^{-1}$  (intense) due to the stretching of O-H, C-H and C-O groups, respectively. The peaks around  $1110\text{ cm}^{-1}$  are assigned to the characteristic C-O-C stretching band in PL appeared at  $1106\text{ cm}^{-1}$  and  $1107\text{ cm}^{-1}$  in the FTIR spectra of **Fig. 3.7(d)** and **3.7(c)**, respectively. The wave number is higher

than the  $1064\text{ cm}^{-1}$  observed in **Fig. 3.7(a)** and **3.7(b)**, attributed to the superposition of C-O stretching vibration of SF and PL in contrast to SF before the addition of PL.

Since Poloxamer is a triblock copolymer of poly(ethylene oxide (A)) and poly(propylene oxide (B)), often denoted by PEO- PPO- PEO, after film blending, the intermolecular hydrogen bonds are formed by interaction between the free hydroxyls group of amino acids (Ser, Asp and Glu) on the SF chain and PEO of PL. The FTIR spectrum of the blend film (**Fig. 3.7(c)**) shows that the amide I and amide II bands of SF at  $1633\text{ cm}^{-1}$  and  $1553\text{ cm}^{-1}$ , shift to approximately  $1631\text{ cm}^{-1}$  and  $1525\text{ cm}^{-1}$ , respectively. This result indicates that the conformation of SF is changed from random coil to  $\beta$ -sheet structure by the addition of PL due to the formation of intermolecular hydrogen bonds between SF and PL (**Fig. 3.8**).

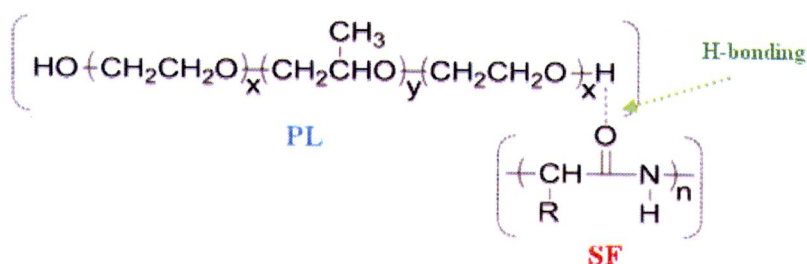


**Fig. 3.8** Intermolecular interaction between SF and Poloxamer

The characteristic IR bands of SF film, SF/PL film and PL powder are summarized in **Table 3.2**.

**Table 3.2** Characteristic IR bands of SF film, SF/PL film and PL powder

| <b>Sample</b>  | <b>Observed frequency<br/>(<math>\text{cm}^{-1}</math>)</b> | <b>Assigned absorption<br/>bands</b> |
|----------------|---|--------------------------------------|
| SF hydrogel    | 1663  | C=O stretching                       |
|                | 1533  | N-H bending                          |
|                | 1239  | C-N stretching                       |
| SF/PL hydrogel | 1663  | C=O stretching                       |
|                | 1525  | N-H bending                          |
|                | 1233  | C-N stretching                       |
| PL powder      | 3495  | O-H stretching                       |
|                | 2885  | C-H stretching                       |
|                | 1106  | C-O stretching                       |

### 3) SF/HPMC hydrogel

If two polymers are miscible, the interactions can shift or change the band intensities and broaden the corresponding vibrations of pure components. The FTIR spectra of the components are shown in **Fig. 3.9** and **Table 3.3**.

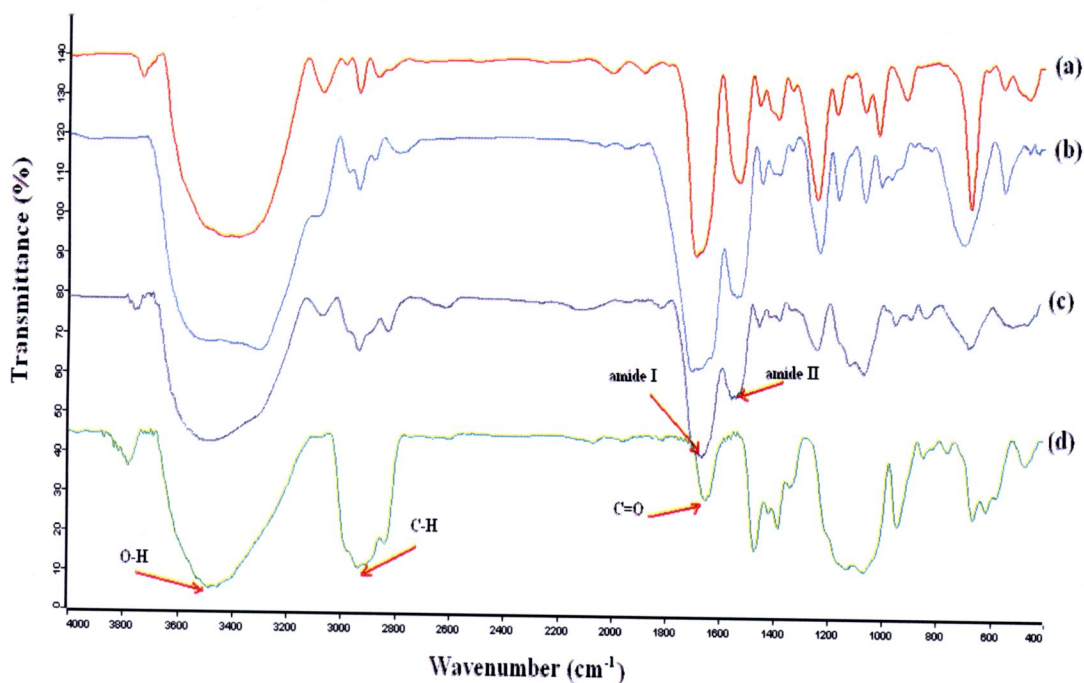


**Fig. 3.9** FTIR spectra of (a) SF powder, (b) SF hydrogel, (c) SF/HPMC hydrogel and (d) HPMC powder

The FTIR spectra of SF, HPMC and hydrogels are shown in **Fig. 3.9**. Pure HPMC (**Fig. 3.9(d)**) has bands related to O-H stretching at  $3448\text{ cm}^{-1}$ , a C-H stretching region at  $3000\text{--}2800\text{ cm}^{-1}$ , C=O carbonyl stretching of the glucose part of the cellulose at  $1653\text{ cm}^{-1}$  and a C-O-C stretching region at  $1300\text{--}900\text{ cm}^{-1}$ . For SF powder which exhibits largely  $\alpha$ -helical and random coil conformations, as indicated by the strong absorption bands (**Fig. 3.6(a)**) at  $1687\text{ cm}^{-1}$  (amide I, C=O stretching),  $1526\text{ cm}^{-1}$  (amide II, N-H bending vibration) and  $1239\text{ cm}^{-1}$  (amide III, C-N

stretching). In case of SF film treated with EtOH, its IR spectrum (**Fig. 3.9(b)**) shows the shifts of the amide peaks at different frequencies of the SF powder. The result suggests that the formation of the SF film after casting and treating with EtOH are changed from  $\alpha$ -helical to  $\beta$ -sheet conformation.

From the results shown in **Fig. 3.9(c)**, the IR spectrum of the SF/HPMC hydrogel exhibits shifts in the absorption bands to  $1663\text{ cm}^{-1}$  (amide I),  $1540\text{ cm}^{-1}$  (amide II) and  $1239\text{ cm}^{-1}$  (amide III) which can be assigned to the  $\beta$ -sheet conformation. The broadening of the band associated with the hydroxyl group indicates the formation of intermolecular hydrogen bonds. These shifts also suggest the formation of intermolecular hydrogen bonding which is similar to the results reported for the blends that form with CP and PL as depicted in **Fig. 3.10**.

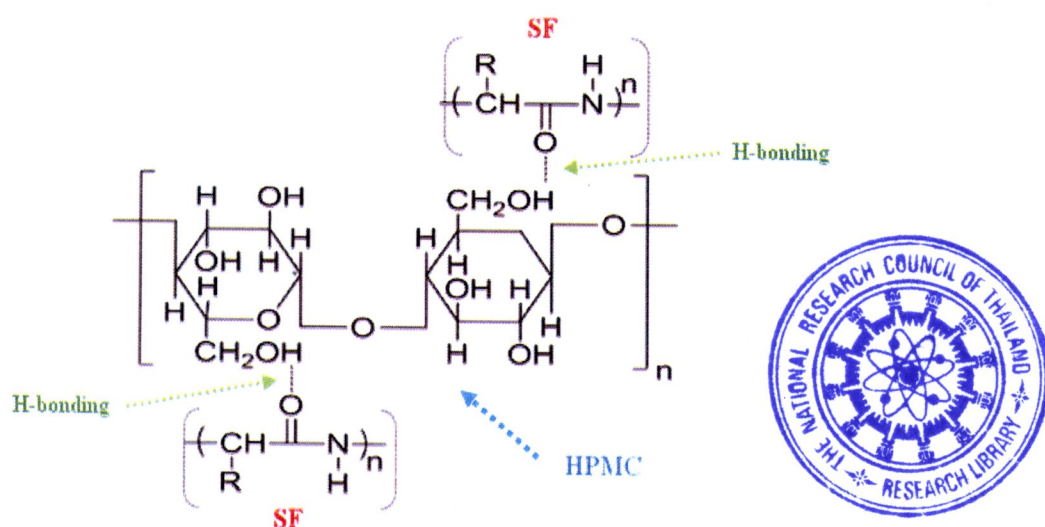


**Fig. 3.10** Intermolecular interaction between SF and HPMC

**Table 3.3** Characteristic IR bands of SF hydrogel, SF/PL hydrogel and HPMC powder

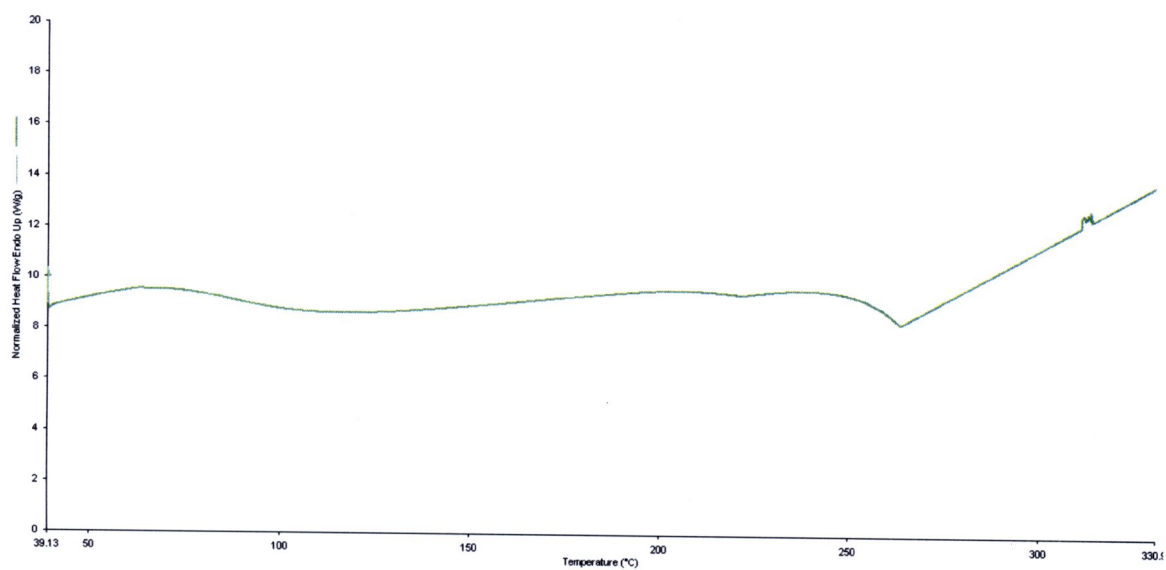
| <b>Sample</b>        | <b>Observed frequency<br/>(cm<sup>-1</sup>)</b> | <b>Assigned absorption<br/>bands</b> |
|----------------------|---|--------------------------------------|
| SF hydrogel          | 1663  | C=O stretching                       |
|                      | 1533  | N-H bending                          |
|                      | 1239  | C-N stretching                       |
| SF/ HPMC<br>hydrogel | 1663  | C=O stretching                       |
|                      | 1554  | N-H bending                          |
|                      | 1239  | C-N stretching                       |
| HPMC powder          | 3448  | O-H stretching                       |
|                      | 2903  | C-H stretching                       |
|                      | 1653  | C=O stretching                       |
|                      | 1064  | C-O-C stretching                     |

FTIR spectra mentioned above will help confirm the effect of EtOH on the introduction of the conformational change of SF. Generally, untreated SF film possesses a structure that is water soluble which becomes less soluble after soaking in EtOH. Actually, water causes the swelling of SF hydrogel that lead to the conformational change from a dense  $\alpha$ - helix form by uncoiling the helices. Once the EtOH seeps into the pores of SF structure, this will cause the rearrangement of inter- and intramolecular hydrogen bonds by converting its structure from random coil to  $\beta$ -sheet. Similar behavior has been reported for treatment with aqueous methanol [45].

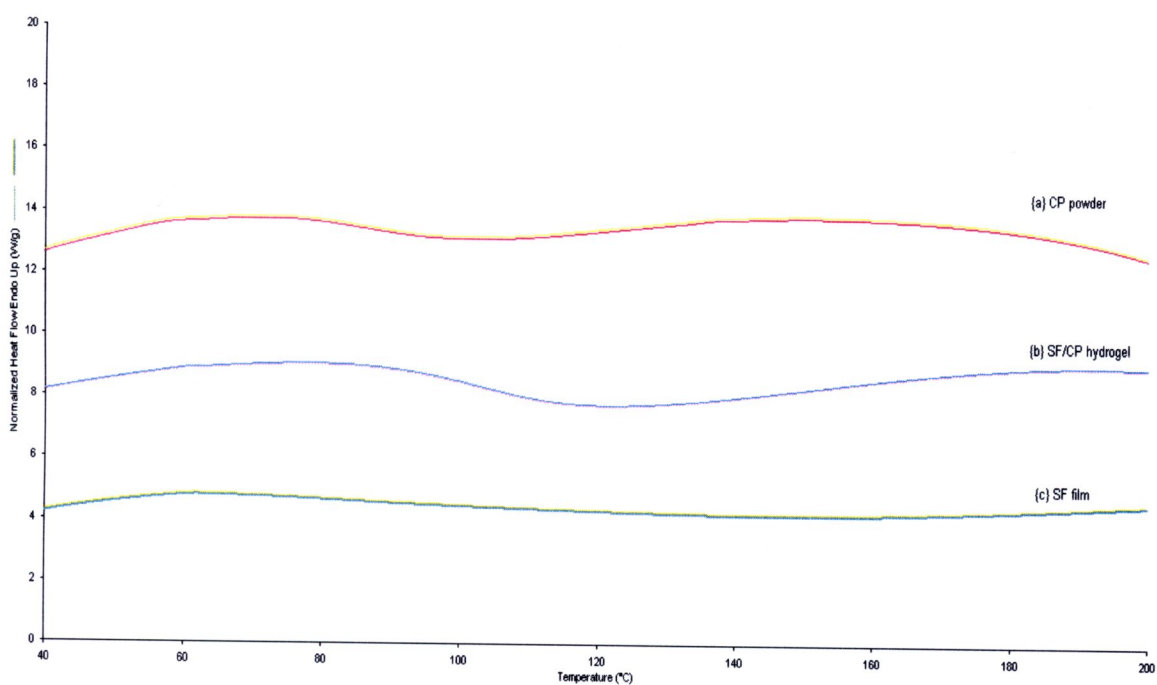
### 3.3.2 Thermal analysis

Thermal properties of the samples were studied with differential scanning calorimetry (DSC) to determine the melting temperature ( $T_m$ ). The measurements were carried out from 40 to 200 °C under nitrogen gas at a scanning rate of 10°C/min. DSC thermograms of pure components and binary composition blends are shown in **Fig. 3.11-3.13**.

Since DSC is aimed to compare the rate of heat flow to the sample and to an inert material which are heated or cooled at the same rate. Changes in the sample that are associated with absorption or evolution of heat cause a change in the differential heat flow which is then recorded as a peak. For proteins, the thermally induced process detectable by DSC is the structural melting or unfolding of the molecule. The transition of protein from a native to a denatured conformation is accompanied by the rupture of inter- and intramolecular bonds, and the process has to occur in a cooperative manner to be discerned by DSC.



a) SF film treated with EtOH



b) SF hydrogels treated with EtOH

**Fig. 3.11** DSC thermograms of (a) SF film treated with EtOH, (b) CP powder, SF/CP hydrogel and SF film treated EtOH (heating rate = 10 °C/min)

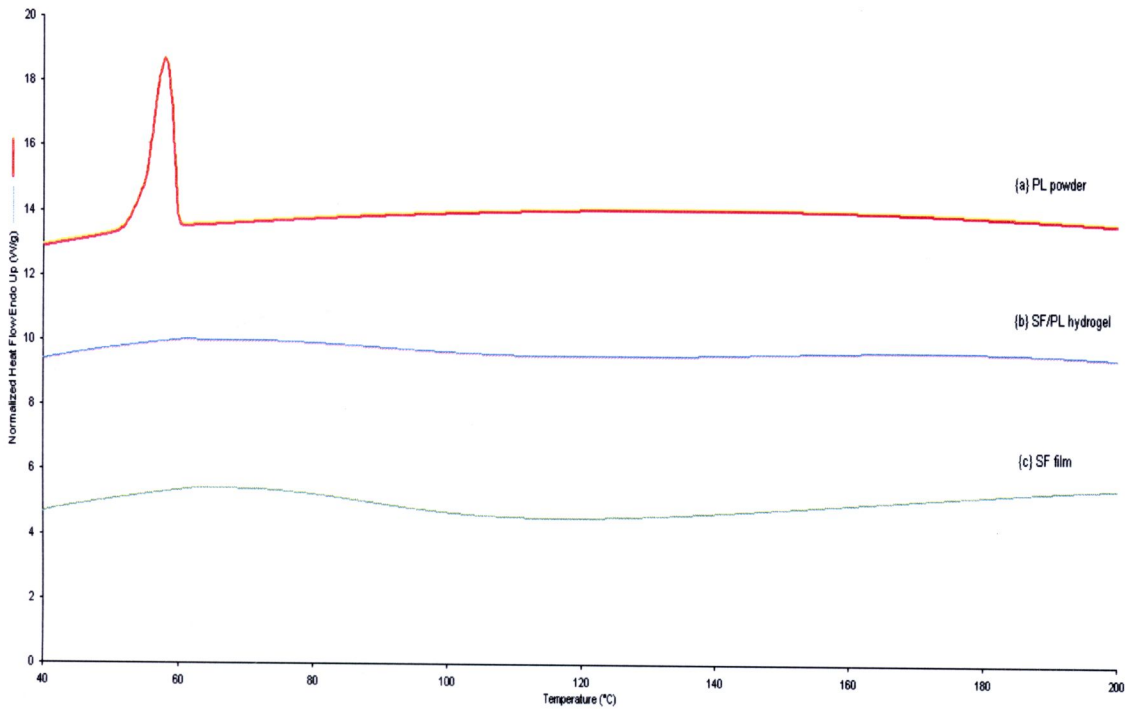


**Fig. 3.12** DSC thermogram of PL powder, SF-PL hydrogel and SF film

(heating rate = 10 °C/min)

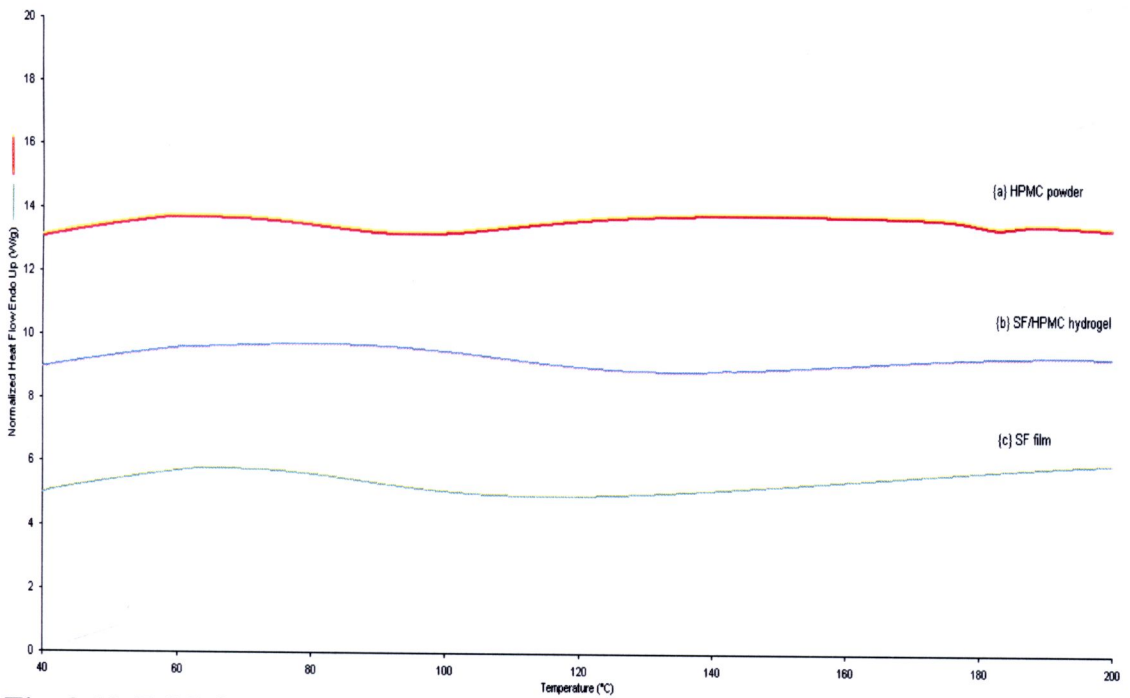


**Fig. 3.13** DSC thermogram of HPMC powder, SF-HPMC hydrogel and SF film

(heating rate = 10 °C/min)

In **Fig. 3.11 (a)**, the DSC study shows that SF displays a water-induced glass state around 87 °C during quick heating, resulting from a temporary bound water-silk structure. After the appearance of crystallization peak at around 222 °C the film immediately starts to degrade, with endothermic peak at around 260 °C. Hu *et al.* [47], also found the glass transition ( $T_g$ ) temperature of SF in SF films at 80 °C, crystallization peak at around 230 °C and endothermic peak at around 260 °C. The endotherms of SF film and SF hydrogels are fairly broad because it is sensitive to water, impurities and crystallinity. The CP powder (**Fig. 3.11 (b)**) shows broad endothermic peak at 103 °C corresponding to the  $T_g$  temperature of Carbopol polymer. Karmarkar reported that  $T_g$  of Carbopol polymers was 105 °C in the powder form [28]. However,  $T_g$  decreases significantly as the polymer comes into contact with water.

**Fig. 3.11-3.13** display DSC thermograms of SF hydrogel films prepared from SF with gel formers. All of the SF hydrogel films have endothermic peaks below 200°C, which might be due to the influence of the moisture. As displayed in **Fig. 3.11 - 3.13(a)**, DSC measurements show broad endothermic peak near 120°C corresponding to the evaporation of water in SF. In **Fig. 3.12**, there is a single and sharp endothermic peak at 58 °C. Chen *et al* [48], also reported that PL 188 was a single and sharp endothermic peak at 54 °C, that corresponded to the melting point of PL 188. From the DSC curve of the SF/PL hydrogel films, the endothermic peak of SF at 120 °C is not observed, whereas the slight transition peak indicates the existence of a mixture as seen in **Fig. 3.12**. The DSC curves of SF hydrogel films showed a broad peak and their melting temperatures appear somewhat different from that of PL.

The DSC endothermic band of pure HPMC powder is shown in **Fig. 3.13**. This band is broad and the  $T_g$  appears at 188 °C. While Wang *et al.* [49] reported  $T_g$  of pure HPMC occurred at 194 °C. DSC thermograms of SF film and SF hydrogels show a wide endothermic band, which can be correlated to the existence of absorbed moisture by the molecule. An endothermic peak attributed to the decomposition of SF film appears at approximately 260 °C. The endothermic melting peak of SF film was observed at 118 °C. The DSC curve of pure PL powder shows a single sharp endothermic peak at 58 °C and the  $T_g$  of PL is not observed due to the PL is a highly crystalline polymer that renders the detection difficult.

Generally,  $T_m$  of a previously crystallized component shifts to a higher temperature subjected to stretching. In other words, when the polymer itself is crosslinked or blended with another material,  $T_m$  increases. The melting point of SF hydrogel is related to the enthalpy corresponding to the energy loss of crystallinity transformation in a process that leads to the decrease in  $T_m$  of SF/PL hydrogel. The small differences are probably associated with the structure and orientation of polymers, residual monomers and polarity (relative hydrophilicity) of polymer molecules. The other factors such as preparation method and heating rate can affect the  $T_m$  values. The shifting value of the melting peaks of SF hydrogels to different temperature confirms the interaction between SF and gel formers.

The results confirm that SF hydrogels prepared from blending SF with different gel formers have enough  $\beta$ -sheet content, which makes these hydrogel water-stable. Thereafter, water molecules become more “free” after their dissociation from peptide chains, which is supported by the conclusion of Hu *et al.* [47]. It was concluded that the bound water molecules in SF film would transform to free water

molecule under heating. Thus, it can be indicated that the formation of  $\beta$ -sheet is related to the dissociation of hydrogen bonds between water and peptide, followed by the re-association between peptides themselves forming stronger hydrogen bonds which made the silk fibroin soluble in water.

Analysis of a DSC thermogram enables the determination of crystallization enthalpy ( $\Delta H_c$ ), the  $\Delta H_c$  value can be calculated from the area under the transition peak. It was correlated with the content of ordered secondary structure of a protein. The  $\Delta H_c$  value is actually a net value from a combination of endothermic reactions and exothermic processes, including protein aggregation and the breakup of hydrophobic interactions [50].

The SF hydrogels samples obtained from SF/CP, SF/PL and SF/HPMC hydrogels showed crystalline endotherms with 443, 111 and 128 J/g, respectively. The peaks of SF hydrogels are integrated to determine the heat of crystallization that corresponding with the expected value of each gel formers. From **Fig. 3.14**, the SF/CP hydrogel film has the highest crystallization enthalpy due to the influences of changing the neutralizing agent of triethanolamine for adjusting the pH of CP gel and CP is a high molecular weight molecule, therefore SF/CP hydrogel film show higher  $\Delta H_c$  value than that of the PL and HPMC. The transition of secondary structure of SF hydrogel film from random coil to  $\beta$ -sheet structure occurred by blending with gel formers. It is considered that gel formers play a similar role of a polar solvent because of abundant polar groups in amino acid composition.

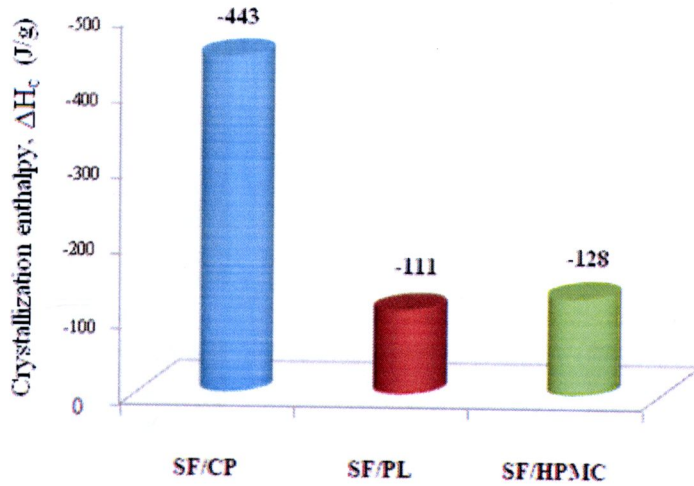


**Fig. 3.14** The  $\Delta H_c$  values of SF hydrogels; (a) SF/CP, (b) SF/PL and (c) SF/HPMC hydrogels

### 3.3.3 Morphology investigation

The cross-sectional morphologies of the samples were observed with a SEM with a JEOL microscope operating at 5 keV with magnification of 5000 at 5  $\mu\text{m}$ . Each treated silk hydrogel was cut into small pieces (0.3 cm $\times$ 0.3 cm) and sputtered-coated with gold in the vacuum chamber to provide a conductive surface. The image was taken in the air, with flattened and plane fitted as required.

**Fig. 3.15** shows the cross-sectional SEM images of SF hydrogel prepared by blending SF with CP, PL and HPMC, respectively. The morphology of the blends with CP and HPMC are more sheet-like compared to that blending with PL. This finding indicates that the gel formers help improve the morphological transition.

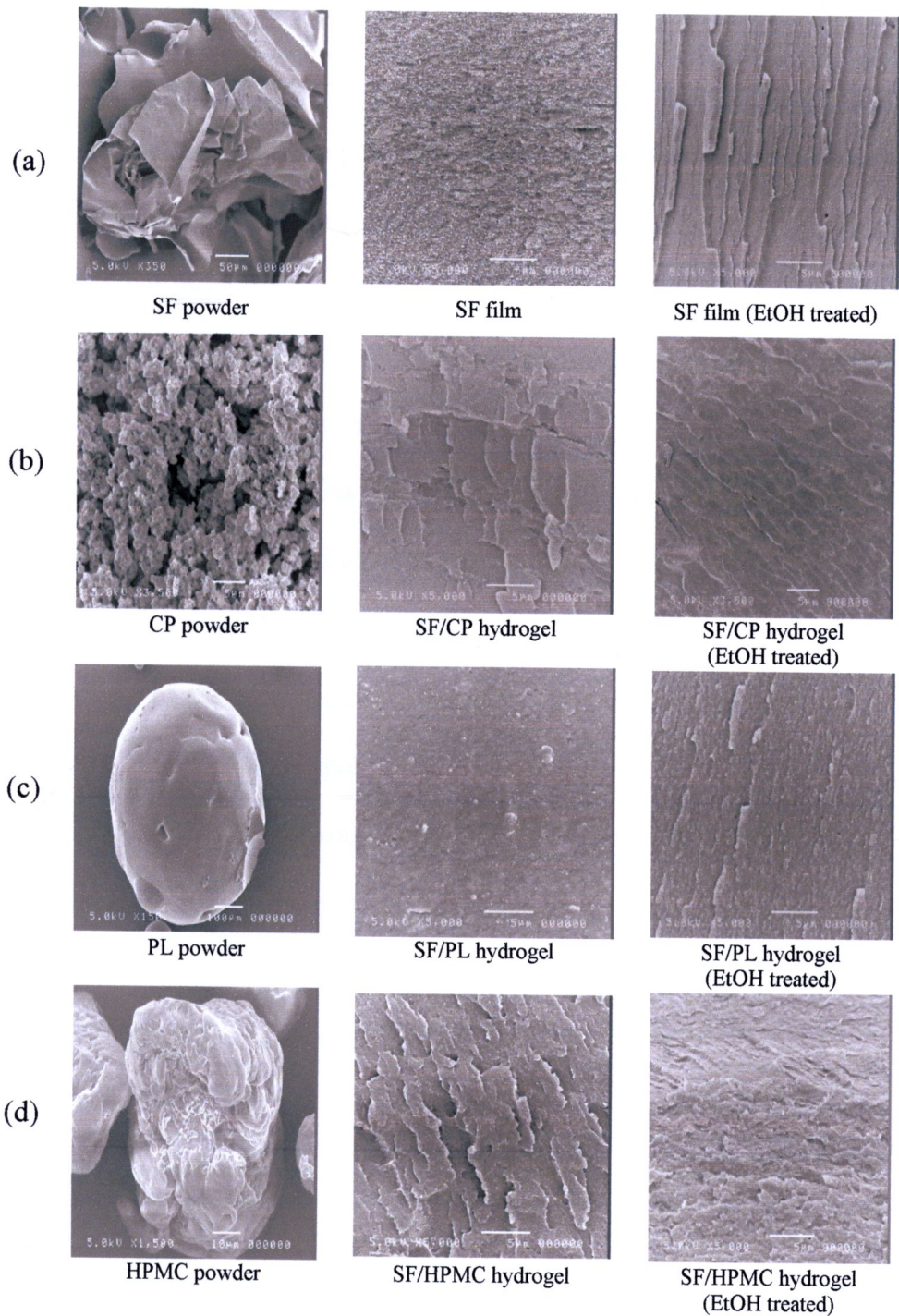
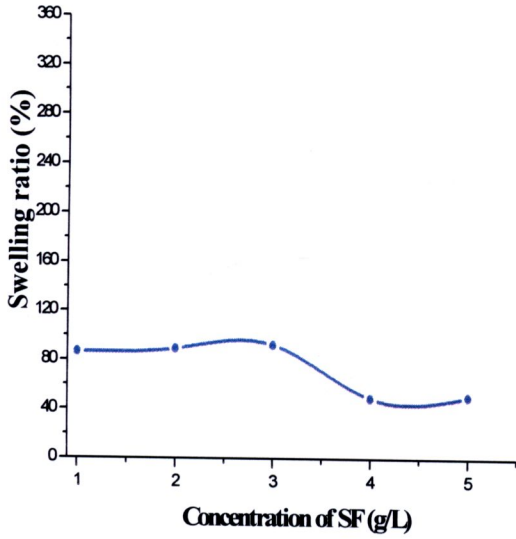


**Fig. 3.15** SEM images of SF hydrogel and gel formers; (a) SF, (b) SF/CP, (c) SF/PL and (d) SF/HPMC

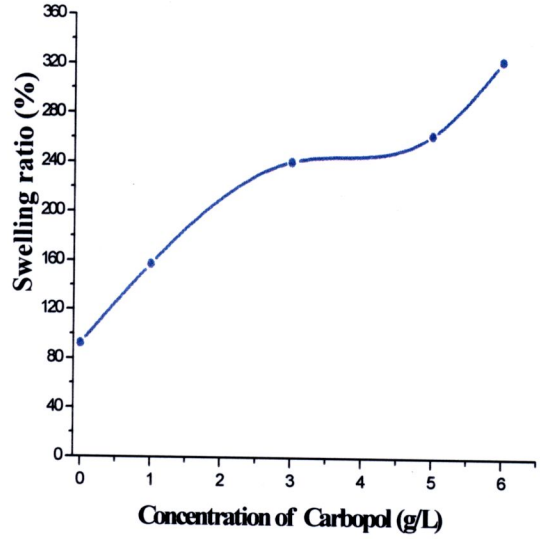
In **Fig. 3.15**, for EtOH treated the SF hydrogel, it can be seen that the cross-sectional structures of the SF hydrogel with added gel formers (**Fig. 3.15(b)-3.15(d)**) become smoother than the pure SF film (**Fig. 3.15(a)**) but the SF film itself exhibits more sheet-like morphology than SF hydrogels. The conformation of  $\beta$ -sheet structure has been reported after treatment with organic solvents such as methanol, ethanol and isopropanol [51]. The conformational change might arise from a dehydration action of ethanol on the random coil of SF molecule, resulting in reorganization of SF conformations to induce intra-or intermolecular secondary bonds. Therefore, it indicates that the possibility of solvent induced SF crystallization in SF hydrogels. When the SF film is immersed in aqueous ethanol, water firstly causes the swelling of the amorphous region of the protein through interruption of hydrogen bonds, then ethanol penetrates the swollen region, generating an hydrophobic environment and making the hydrophobic molecule chain segments in the random coils of SF to get closer to each other and form a crystal nucleus. Finally, stable  $\beta$ -sheet conformation is formed by the growth of crystal nucleus and rearrangement of hydrogen bonds [45].

#### 3.3.4 Swelling test

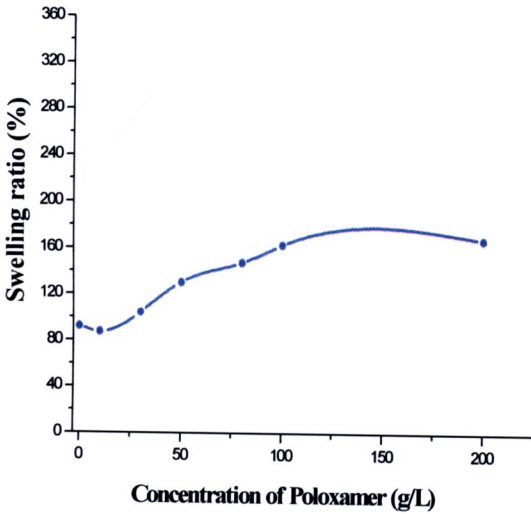
The swelling ratio of treated SF films and SF hydrogel films were determined from the weight change of the films, after soaking in water. The weights of dried and swollen films are summarized in **Fig. 3.16**.



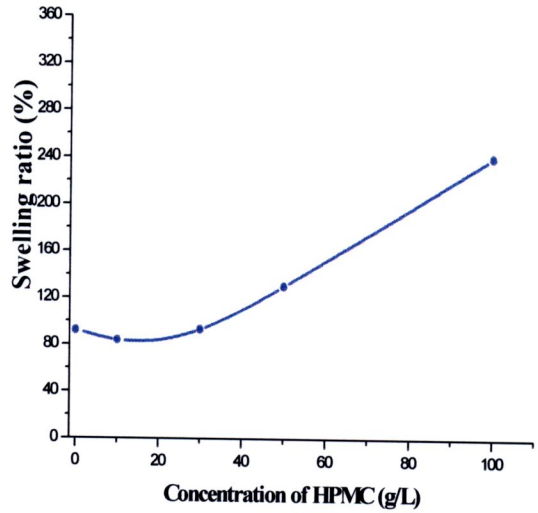
(a)



(b)



(c)



(d)

**Fig. 3.16** The swelling ratio of (a) SF hydrogel, (b) SF/CP hydrogels, (c) SF/PL hydrogel and (d) SF/HPMC hydrogels

The SF solutions at 10-50 g/L wt were poured into PE plate as described in section 2.3.1. Generally, the SF films were transparent and yellowish. After treating

with EtOH, the films 10-50 g/L were rigid and brittle. Evaluation of the percent swelling ratio of SF film in water are described in **section 2.3.1.3** and shown in **Table 3.2-3.4**. Details of the calculation are shown in **Appendix A**.

The swelling ratios of SF films at various concentrations are shown in **Fig. 3.16(a)**. Once the SF was mixed with each gel former at different concentrations, the swelling ratio of the hydrogel from start increasing from the maximum value which is approximately 90% (**Figs. 3.16(b)-3.16(d)**).

The swelling data in **Fig. 3.16(b)** clearly demonstrates that % swelling ratio increases drastically with the increase of CP content in silk fibroin hydrogel. Once wet, CP swells quickly causing high viscosity, mostly below 10 g/L. The crosslinked polymers are not actually water soluble, but swell into hydrated spheres that improve its rheological properties. In addition, the swelling ratio of SF/CP hydrogels increases faster than those of SF/PL and SF/HCMP hydrogels when the concentration of gel former increases. This happening may arise from the reason that SF/CP hydrogel also contains triethanolamine (TEA). As discussed earlier that TEA acts as a spacer in the blend (**Fig. 3.6**), therefore more pores are created in the blend network causing higher capability of the SF/CP hydrogel to imbibe more water.

In **Fig. 3.16(c)**, the swelling ratio of SF/PL hydrogel films increases when the concentrations of PL are between 10-100 g/L and becomes almost constant later. So, the optimal concentration of PL for hydrogel blend formation is 100 g/L. Likewise, the degree of swelling ratio of SF/PL hydrogel films was nearly constant when concentration of PL higher than 100 mg/mL. The swelling kinetics can be generally described in two terms; the diffusion rate of solvent imbibing into the gel and the relaxation rate of polymer network. Therefore, it indicates that increasing

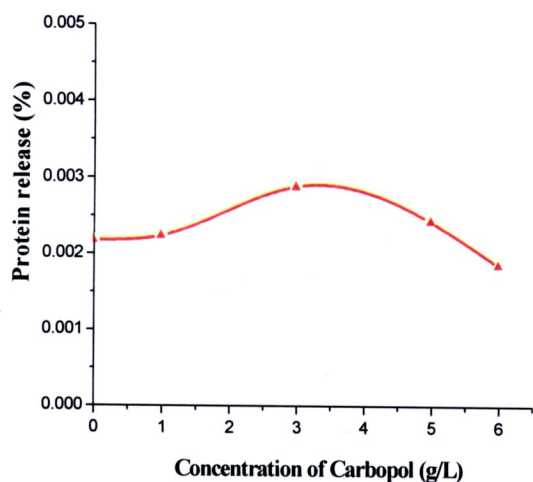
polymer content may attribute to an increase of cross-link density in hydrogel. But high concentration can interrupt the relaxation of polymer network, resulting in an obstruction of their swelling behavior. Moreover, the increase of swelling ratio could indicate the interaction of hydrophobic PL in SF hydrogel [22].

In **Fig. 3.16(d)**, the swelling ratio of SF/HPMC hydrogel films at concentration more than 30 g/L also increase sharply. This may be due to the cross-linking makes SF chains covalently link together and form network of the hydrogel films even though it restricts the swelling ratio of hydrogel films. Besides, HPMC has a glucose-like structure of cellulose that can bond with SF protein causing a larger size structure. If this type of structure in SF/HPMC hydrogel becomes swollen in water, it can expand the size enormously and accommodate more water molecules resulting in the increase of swelling ratio.

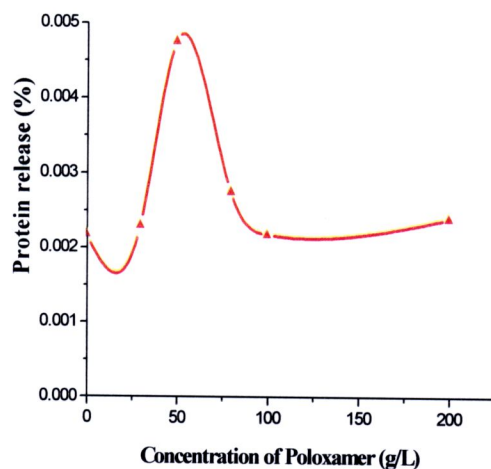
Therefore, results of the swelling ratio, (**Fig. 3.16**) can be concluded that the swelling is dependent on the content of each gel former in the SF hydrogel films; SF/CP hydrogel shows the highest swelling behavior because it had the highest hydrogen bonding among Carbopol, triethanolamine and SF. When the SF/CP was exposed to water, the polymer was uncoiled generating an increase in viscosity and gel formation. In the case of SF/PL hydrogel, the hydrophilic parts of the poloxamer absorbed water around the SF molecules and the conformational change of SF from random coil to  $\beta$ -sheet structure was accelerated by addition of poloxamer [22]. Whereas, the swelling ratio of SF/HPMC hydrogels increased with increasing content of hydroxypropyl group in HPMC and amino acid group of SF. The reason is consistent with our results that water absorption of SF film itself which is low and gel formers can improve the water absorbability of SF.

### 3.3.5 Protein loss detection

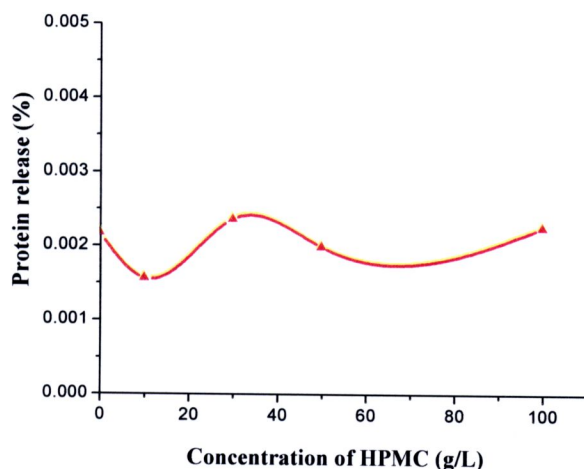
Hydrogels are stabilized by cross-links between the polymeric units that form the backbone of the gel, these bridges may be H-bonding. Protein release behavior can be attributed to a combination of protein diffusion and polymer degradation. When SF hydrogel is immersed in excess water, the gels first swells and then starts to degrade. The loss of SF protein from SF/gel former films was determined by measuring the absorbance of solubilized SF protein at 275 nm in DI-RO water (solution from **2.3.3A**). Then, the quantity of the SF released was determined from the absorbance of the equilibrated solution using a UV-VIS spectrophotometer at the optimum wavelength (see **Appendix B**). The calibration graph of SF solution is shown in **Appendix B**. In **Fig. 3.17**, the percentage of SF loss from treated SF hydrogels with gel formers were also compared by measuring its absorbance at room temperature at the same optimum wavelength.



(a)



(b)



(c)

**Fig. 3.17** The protein loss of (a) SF/CP hydrogels, (b) SF/PL hydrogel and (c) SF/HPMC hydrogels

In **Fig. 3.17(a)**, the % protein release of SF/CP hydrogels reaches maximum at 3 g/L and slowly decrease thereafter.

**Fig. 3.17(b)** displays the protein release from the SF/PL hydrogel. However, the protein release (%) increase from 10-30 g/L and remained constant

afterward, after that gradually increased again to increasing concentrations of gelling agent visit. The increase of Poloxamer content may cause an increase of cross-linking density in the hydrogel. But high concentration can interrupt the relaxation of polymer network, resulting in an obstruction of their swelling behavior. The reason that SF/PL hydrogels having the highest protein release is because when the hydrogel is swollen in water, its configuration will be stretched and the crosslinkage between SF and PL will become weaken. Thus making the protein be easily lost.

In **Fig. 3.17(c)**, the % protein release pattern of SF/HPMC hydrogels are nearly the same as of SF/CP hydrogels where the HPMC concentration at 30 g/L exhibits the greatest release of SF protein.

The protein release of SF/Gel former hydrogels after treating with 80% EtOH at room temperature as a function of gel former concentration is illustrated in **Fig. 3.17**. It was found that the protein release of SF from SF films after ethanol treatment is 0.022 % and the protein release from SF/PL hydrogel was more than that released from the other gel formers studied. When the SF film is immersed in ethanol, water firstly forms the hydrogen bonds with the SF, swells the amorphous region of the protein through the competition with the inter-intramolecular hydrogen bonds existed in the SF, then the ethanol penetrates the swollen region, generating hydrophobic environment and making the hydrophobic molecule chain segments in random coils of SF get close to each other and form crystal nucleus. Finally, stable  $\beta$ -sheet conformation is formed by growth of crystal nucleus and rearrangements of hydrogen bonds [46].

The relationship between the amount of SF release and swelling ratio at various concentrations of SF hydrogels are shown in **Fig. 3.18**.

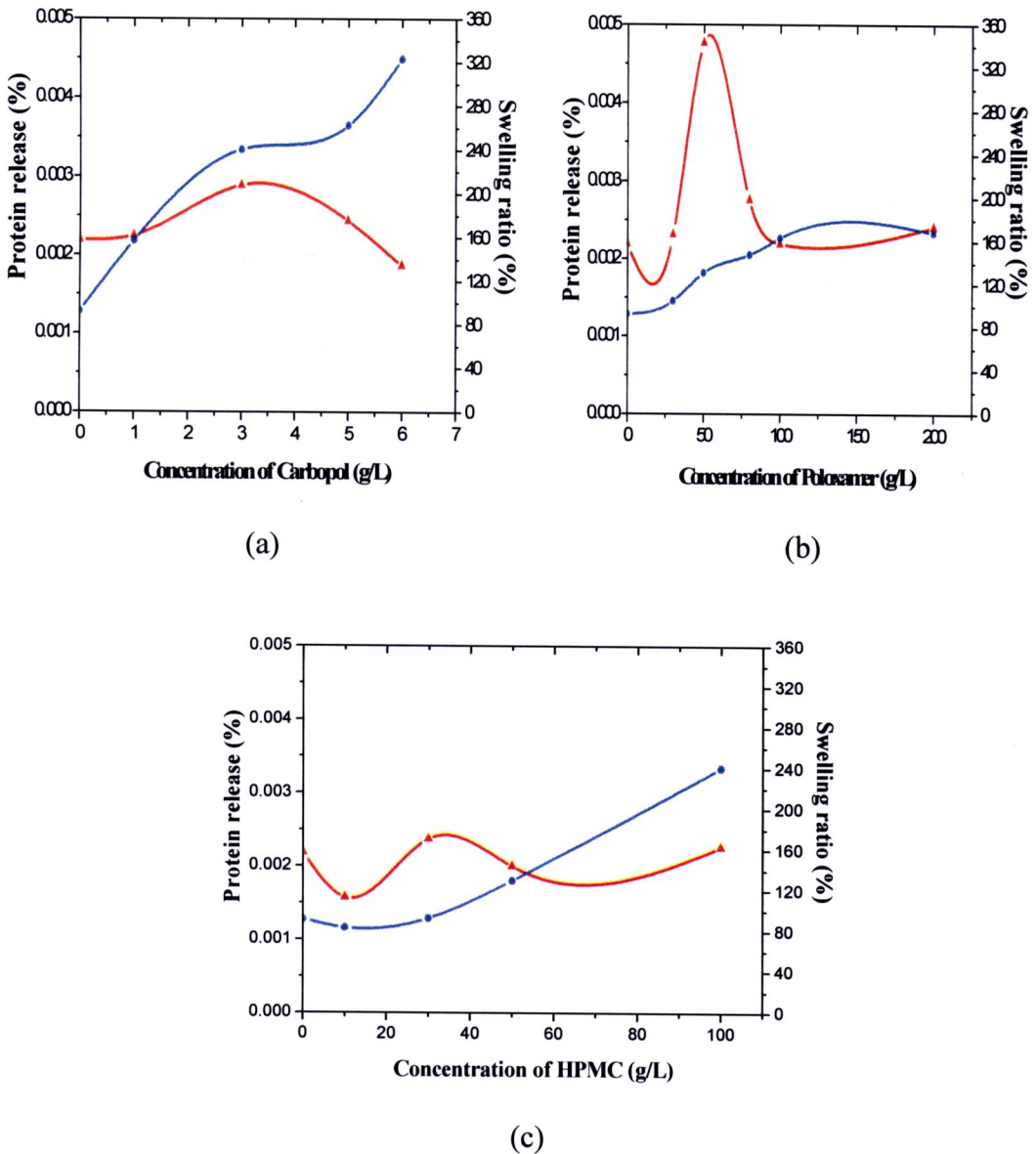


**Fig. 3.18** Relationship between swelling ratio (-●-) and protein release (-▲-) with various concentrations of CP (a) SF/CP hydrogels, (b) SF/PL hydrogel and (c) SF/HPMC hydrogels

In **Fig. 3.18**, can be clearly seen that the swelling and protein release properties of cross-linked SF hydrogels depends on the crosslinking agent

concentration and pH. Because, the polymer swelling is a process that the polymer structure stretch itself to release the stress.

As a conclusive picture, it is understandable that the protein release occurs due to the interaction of water molecules that penetrate into the hydrogel structure. The lower which result in the concentration of the gel former; the more penetration of water molecule occurs the more rupture of the hydrogel network. On contrary, at higher concentrations of the gel formers, the network of hydrogel is so strong that even more water molecules can penetrate the hydrogel structure causing high swelling ratios but the rupturing of the network becomes less resulting in the lowering of SF protein release. This phenomena is clearly illustrated in **Fig. 3.18** for all cases of hydrogel under study.